# Environmental information extracted from satellite images: Aspects of Sea and Atmosphere

Tomoo AOYAMA[1), Toru YAGI[1)

Abstract

To extract environmental information from published satellite pictures, computer approaches are discussed. Satellite images are given as time-series multi-spectrum bands, and include many phenomena. To analyze a target event, others must be eliminated. The approaches are projection, compositing, intensity-ordering hold non-linear transformations, etc., which are defined by mathematical expressions. We apply them to see hue changes on the sea surfaces, and to detect reactions in the air between dust and moisture. Processing images get significant in relations with environmental knowledges and experiences.

**Keywords:** composite, time-axis accumulation, sea current, sea vortex, eutrophication, nutrient salts, Japan Sea, East China Sea, Kuroshio

## 1. Preface

There is a satellite, Himawari-8, at location (140.7 [deg] east longitude (E), 0.0 [deg] north latitude (N), 35793 km height) [1]. Scanning information on the earth is processed, and time-dependent images for 16 bands in 0.47~13.3 $\mu$m are published. In these images, general purpose ones of portable network graphics (png) format are as a data base [2] with a viewer [3]. Using the viewer, environmental pre-events on the target area can be detected. It is an important function to pick up a signify presage from sea of meaningless events.

There are two download links, Japanese Archipelago and the globe, in the viewer. From those links, educational pictures can be got, that are very superior to see Typhoons vortices, front lines, and seasonal winds. There are information about suspended particulate matter (SPM), black mist haze, sea surfaces, and vegetation, also. They are weak images; thus, they are detected by extracting from main patterns strongly. Our aims are to show the extracting methods.

## 2. Processing for the whole image

Png-format images have RGB components of 8-bits, which are read as 1-byte unsigned integer in Fortran/C programs, and stored in arrays as 32-bits floating point data. We write the arrays in notation, {Rij, Gij, Bij}. If meteorological images are used for other purposes, they have not sufficient signal-noise (S/N) ratio. We accumulate N-images; thus, the ratio is reduced to $-20\log(N^{-0.5})$ [db]. This is a composite processing for still images. In case of moving images, we introduce another approach that is followings.

### 2.1 Digitizing of movements in Himawari-8 images

One pixel of Himawari-8 is 1 km; therefore, velocity is x [m/s], and time is T [min], the trace length, L, is L=*int*(60Tx/1000) [pixel]. The *int*() is a rounding up function. The T is 2.5 or 10 min for Japan or the globe images [2]. The brightness of moving objects is 1/L, thus; the image of a moving isolated cloud becomes low brightness. This is an acceptable effect. But, images of large scale clouds keep the brightness, the effect is limited.

### 2.2 Enhancements of the color

Strong brightness objects are clouds. Since it is so brighter than others, you must reduce the brightness. We desensitize white components of pixels.

W=*min*(Rij, Gij, Bij), Rij'=Rij-Wf,
Gij'=Gij-Wf, Bij'=Bij-Wf, 0≤f<1, (1)

The "f" is a parameter how to express cloud. At same time, it enhances the colors of whole objects. We use f=0.5 as a default. So, haze around clouds become like a dark mist. Eq.(1) makes white-clouds be colors. If you think that the effect is inappropriate, reduce the f-value as 0.5→0.25→0.125. The {Rij', Gij', Bij'} image is dark, in which the color is emphasized. Hereafter, we write this image again as {Rij, Gij, Bij}.

The difference part between each color is same in Eq.(1). A {R'G'B'}-image is reduced brightness, whose

2019年1月30日受付　2019年2月6日受理
1) Edogawa Univercity Institute of Information Education

effect makes images towards grayish. The screen impression gets dark. So, we raise the a-value (cf. Eq.(2)) and make it brighter. Where, "R'~R, G'~G, B'~B". Therefore, the difference part is enlarged. That makes the color emphasis.

### 2.3 Suppress of bluish tones

Almost satellite images are bluish, and visibility of target objects is lower. It should be corrected. The center RGB wavelength for digital cameras is 0.63, 0.55, 0.45 μm, which is enacted to resemble human vision. We let the wavelength be λr, λg, λb. RGB component ratio of the reflected luminance of particles is $\lambda r^n$: $\lambda g^n$: $\lambda b^n$, n=-4, in ideal Rayleigh scattering. In Mie scattering, the n is 0. Therefore, in order to correct a blue foggy image, the n-value is defined, and the pixel's values must be multiplied by $\lambda^{-n}$. We use n=-2 [5] in Japan, n=-2.5 in the whole globe.

Converted images are dark as it is, almost invisible. To visualize them, we introduce coefficients and a function.

x=a Rij-b, y=g(x; u)=255/{1+*exp*{-u(x-127.5)}},

Rij'=255(y-0.44464)/254.13,

IF(Rij'>255)Rij'=255, and IF(Rij'<0)Rij'=0, (2)

Let Rij' be Rij again. The same re-notation applies to Gij and Bij. Eq.(2) needs to determine a parameter u for increasing contrast at middle point of brightness. We adopt u=0.05. Since threshold logic is adopted, it is always 0≤Rij≤255. The same applies to Gij and Bij. Eq.(2) is a type of Sigmoid functions, which is a nonlinear transformation but retains the ordering of amplitude of brightness and is effectively linear in a central part of the [0,255] section. This property is essential for scientific images. Since the density relates brightness normally, the linearity should be hold.

### 2.4 Tone emphasis and correction of brightness gradient

Variable "a" of Eq.(2) is an amplify factor, which is $\sim N^{0.5}$ in random noises. The "N" is the number of accumulation images. Using $a>N^{0.5}$, it is excess amplification; so selection of b-factor is important. The b-factor moves a brightness center of targets towards 127.5-brightness value. The target must be determined by users. The center brightness value is optimized by the interactive RGB-viewer.

If one variable is used for the b-factor, on excessive amplify, the brightness-gradient is arisen for horizontal and vertical directions. It should be corrected. The number of whole pixels for horizontal/vertical direction is N/M, respectively. We set brightness gradients that are dx and dy, in interval [0, 255]. Here brightness is that of the background, but it is not for individual objects. Since it is not the brightness of a target object, dx and dy are not determined clearly. While looking at the whole screen with a viewer, decide the dx and dy values to make adjustments for left and right, top and bottom.

Two functions, bE() and bN(), are defined as;

bE(i)=(dx/N-1)(i-1), bN(j)=(dy/M-1)(j-1), (3A)

Using Eq.(3A), we define 2 Affine-transformations; these are;

x=a Rij-b+bE(N-i), y=a Rij-b+bN(M-j). (3B)

The transformations are corrections for brightness-gradients. Thus, "b"-factor is a vector {b,dx,dy}.

### 2.5 Digital gradation filter

When outlines of the earth appear in images, the atmosphere illumines blue. It is difficult to correct linear bias approaches in section 2.4. The following nonlinear luminance correction is introduced and we call it digital gradation filter, DGF(i,j).

RH=5473, RV=5425, Y(j)=RV-j, 0<j<RV, X(i)=i, 0<i< RH,

$R(i,j)=(X(i)^2+Y(j)^2)^{0.5}$, $DGF(i,j)=\{1-R(i,j)/L(j)\}^{1/3}$,

where, L(j)=RH-j(RH-RV)/RV, (3C)

An operation of DGF() is Rij=Rij*DGF(i,j), in which the operation applies to Gij and Bij. RH and RV values are pixel numbers that are got from the global image. A parameter exponent 1/3 is determined empirically. The filter is applied near the edge of global pictures; there is no meaning for Japan area.

## 3. Partial imaging process

### 3.1 Threshold logic

The former processing cannot reduce large scale clouds. If the clouds move within a relatively short time, and if phenomena in lower layer appears; we have a chance to detect them. To see tiny phenomena near high brightness clouds, we use a binary logic function *L*(), which is defined a threshold set {thR, thG, thB}.

*L*{(Rij>thR) and (Gij>thG) and (Bij>thB)}=.True., (4A)

Forced to set Rij=Gij=Bij=0, in *L*()=.False.. (4B)

Non-integrated pixel is arisen; therefore, an integration number is held for each pixel. Average pixel values are calculated from the numbers. The S/N ratio is -20log{aver age(accumulation#$^{-0.5}$)} [db]. The thresholds {thR, thG, thB} is determined from a histogram of whole pixels. An example is **Figure 1**, which is an aspect of clouds. Where, the boundary around clouds cannot be detected clearly. On such a condition, we must introduce the threshold logic.

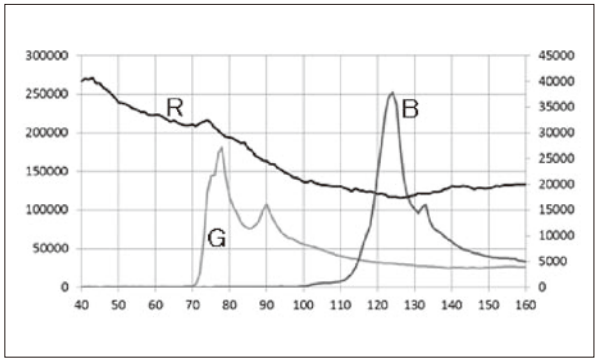


**Figure 1. RGB histogram of an accumulated for 49 images of Japan Archipelago, which are got per 2.5 min from 9:00 to 11:00, in July 16, 2017.**

Right vertical axis: the pixel numbers for Rij; Left vertical axes: the pixel numbers for Gij and Bij. Horizontal axis: the brightness values of pixels. R-, G-, and B-curves are for Rij, Gij, and Bij elements, respectively.

We interpret the histogram as followings; 3 small peaks on high brightness side for RGB curves mean the cloud. Based on the interpretation, {thR, thG, thB} is {71, 86, 132}. If "n=-2.0" in the discussion of section 2.3 is used, we get {71, 112, 132}. The difference for "thG" is arisen from that RGB wavelength of Himawari-8 is 0.47, 0.51, 0.64 $\mu$m. The visual image of Himawari-8 is not as that of human vision; certainly it is different. The satellite image is optimized for separating phenomena clearly. Considering the clouds simply, a relation, thR~thG~thB, is accepted; but it is inappropriate. The clouds are bluish in the satellite images.

### 3.2 Compositing along time-axis

Introducing a logical function and partial imaging, composite process is changed as;

$$Mij=\Sigma t=0{:}N\ 1\times L(\text{true: Rij} > \text{thR}), \quad (5A)$$

$$\text{Rij}(0)=[\Sigma t=0{:}N\text{Rij}(t)\times L(\text{true: Rij} > \text{thR})]/Mij, \quad (5B)$$

$$\text{Rij}(1)=[\Sigma t=0{:}N\text{Rij}(t)\times L(\text{true: Rij}>\text{thR})\times\{2mod(t,2)-1\}]/Mij, \quad (5C)$$

$$\text{Rij}(2)=\text{Rij}(0)-\text{Rij}(1). \quad (5D)$$

Operation ($\Sigma t=0{:}N$) is summation that is from t=0 to N (equidistant time can be expressed by integer index). The attached condition of Eq.(5C) is N=*even*. Rij(t) is Rij at time t. $L$(true: Rij> thR) is binary logical function, which is 1/0; *i.e.*, .true./.false. The same is true for Gij(t) and Bij(t). Eq.(5B) gives a conventional composite approach; and Eq.(5C) erases stillness objects. Eq.(5D) emphasizes stillness, and stripes moving objects. When N is small number, there is no effect of Eq.(5D); and Eq.(5B) is recommended. When original images are a few, it is necessary to relax the condition of $L()$. This is a practical integration.

Since there is a chopper function in under line part of Eq.(5C), an extended form is considered.

$0\leq t$, $\sim\{2mod(t,2)-1\}=\{1-2mod(t,2)\}$, the expression is same as infinite multivalued logic ~x=1-x (~ is an operator).

Since "t" is an integer greater than or equal to 0, we can also use Eq.(5C) as $\{2mod(t1,2)-1\}$ by introducing $t\rightarrow[t/2]\equiv t1$. If we write the chopper function as Rij(1;t1);

$$\text{Rij}(2E)=\text{Rij}(0)-\sim\text{Rij}(1)-\text{Rij}(1;t1), \quad (5E)$$

We examine whether these formulas have effects on objects whose cloud-like contour changes step by step. We select one dimensional Gaussian model, GM(x). Where the "x" is the model space, x={0,1,..100}, which is represented by discrete vector, corresponding with [pixel]. The expression of GM() is;

$$GM(x)=\Sigma_{t=0,10}\ G(x,A1,tv1)+G(x,A2,tv2),$$

$$A1=2\times10^{-2},\ A2=4\times10^{-3},\ G(x,A,c)=\exp\{-A(x-c)^2\},$$

$$v1=8,\ v2=0. \quad (5F)$$

The "t" corresponds with the time, which is set integer in period [0,10].

Results of Eqs.(5D,5E) are shown in GM(x) model for moving and fixed Gaussians, which have equal intensity and non-diffusion.

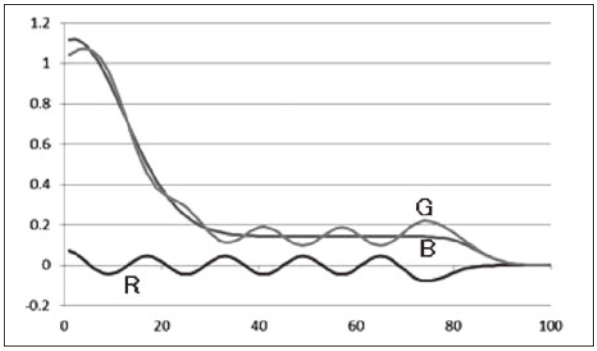


**Figure 2A. Gaussian values from Eq.(5D) and GM().**

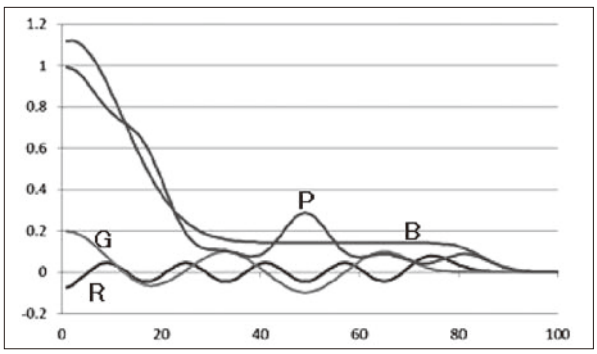


**Figure 2B. Gaussian values from Eq.(5E) and GM().**

Vertical axis is Gaussians sum values. Horizontal axis is argument values in the exponent of 2 Gaussians that mean a distance between 2 Gaussians.

In case of figure 2A, B-, R-, and G-curves are calculated from Eq.(5D), Rij(1), Rij(2), respectively.

In case of figure 2B, B-, R-, G-, and P-curves are calculated from Eq.(5E), ~Rij(1), Rij(1;t1), Rij(2E), respectively.

In Eq.(5D), it is enable to judge stillness or moving for Gaussians. The still-Gaussian is seen as a Gaussian-form, in other hand, the moving one is stripe band pattern. Although, 2D phenomenon makes complex stripe patterns; because of existence of convection and diffusion. We may see phenomena expressed by Navier-Stokes equations, which would be contour patterns. In Eq.(5E), the moving part attenuates more than (5D), but resonance is arisen. It is difficult to adopt it due to the side effects.

## 4. Relation among GPS coordinate and pixel location

Examine the X/Y pixel values and latitude/longitude values of typical geographical features on an image, and calculate an approximate function with excel. We get following relations for Japan area.

$X=100.0168E -11901.4108$, $R^2=0.999993$,

$Y=-100.1531N+4855.6764$, $R^2=0.99998$, (6A)

$E=0.009998247X+118.9942$, $R^2=0.999993$,

$N=-0.00998451Y+48.4823$, $R^2=0.99998$, (6B)

Where, the units of {X,Y} and {E,N} are pixel number and [deg]. The E/N is latitude/longitude. Precision of Eqs. (6A,B) is O(-5), which is sufficient for images of O(3) pixel numbers.

As for the whole globe image, the former approach gives not so reliable. We get following relations, whose precisions are O(-3) for X, and O(-4) for Y. They can be used in the area of E=130~170 [deg] and N=25~40 [deg].

$x=E-140.7$ [deg],

$X=0.08418376x^2-89.32120110x-5.37821750$, $R^2=0.992$,

$y=N$ [deg], $dX=-0.0664y^2+7.9454y-182.51$,

$z=E$, $d^2X=-0.0186z^2+5.2212z-362.52$,

$X_{revised}=(11000/2-3399)-(X+dX-d^2X)=f(E,N)$, (6C)

$Y=0.64583426N^2-126.69146453N+4647.8402698$, $R^2=0.9990$,

$dY=0.0693E^2-19.424E+1349.1$,

$Y_{revised}=Y+dY=g(E,N)$, (6D)

We use a blank map approach for other regions. The map is got by digitizing the coastline, which is in night image of Himawari-8 viewer. Magnification ratio for displayed image is maximum, and by using the screen copy a Png-file is got;

**Figure 3. An blank map (3301×2701 pixel) for the Okhotsk area.**

where conversion ratios between the magnification and down load images are 1.00380 and 0.99783 for X and Y directions. Those values can be used for checking a digitizing cording. **Figure 3** is a blank map of Okhotsk area.

## 5. Verifications

To research movements of substances, we detect color changes of the Japan Sea, the East China Sea, and Kuroshio in the Pacific Ocean. The former 2 are for investigation of aspect of Tsushima and Liman currents, and later is for interactions between Kuroshio and Oyashio currents. Due to printing costs, color images are converted to monochromes. Thus, the eutrophied ocean is drawn white.

### 5.1 Japan Sea

The Japan Sea has cross-sectional shape like a deep bowl, which has 4 entrance/exits and complex currents. Traditional knowledge of sea currents is Tsushima and Liman ones [4]. The reference gives currents based on heat flows. However; as substances, they interact on each other in the sea, and make complex convection-diffusions field. We wish to detect the field. We show a surface image of the Japan Sea in **Figure 4**, which is detected trough SPM and haze. The GPS list for the section is in **Table 1**.

The Figure includes clouds, SPM, sea surfaces, and undeleted scan lines. Clouds are black (using section 3.1; {thR,thG,thB}={46,72,85}). The SPM patterns are stripes by section 3.2. “N” of Eq.(5B) is 49, and “f”-factor of section 2.2 is 0.5, and “a,b” of section 2.4 is “10, {-380,0,-135}”. The eye-power is about 7 times stronger than human.

Considering **Figure 4**, we point out as followings;

(1) Liman current is not detected visually. It is weak at the spring in 2018.

(2) Tsushima current is weak, but it exists certainly along coast of Japan. It is not a river in the sea. It has many vortices, which indicates the rough sea. Both currents are observed at a sea-observatory [5].

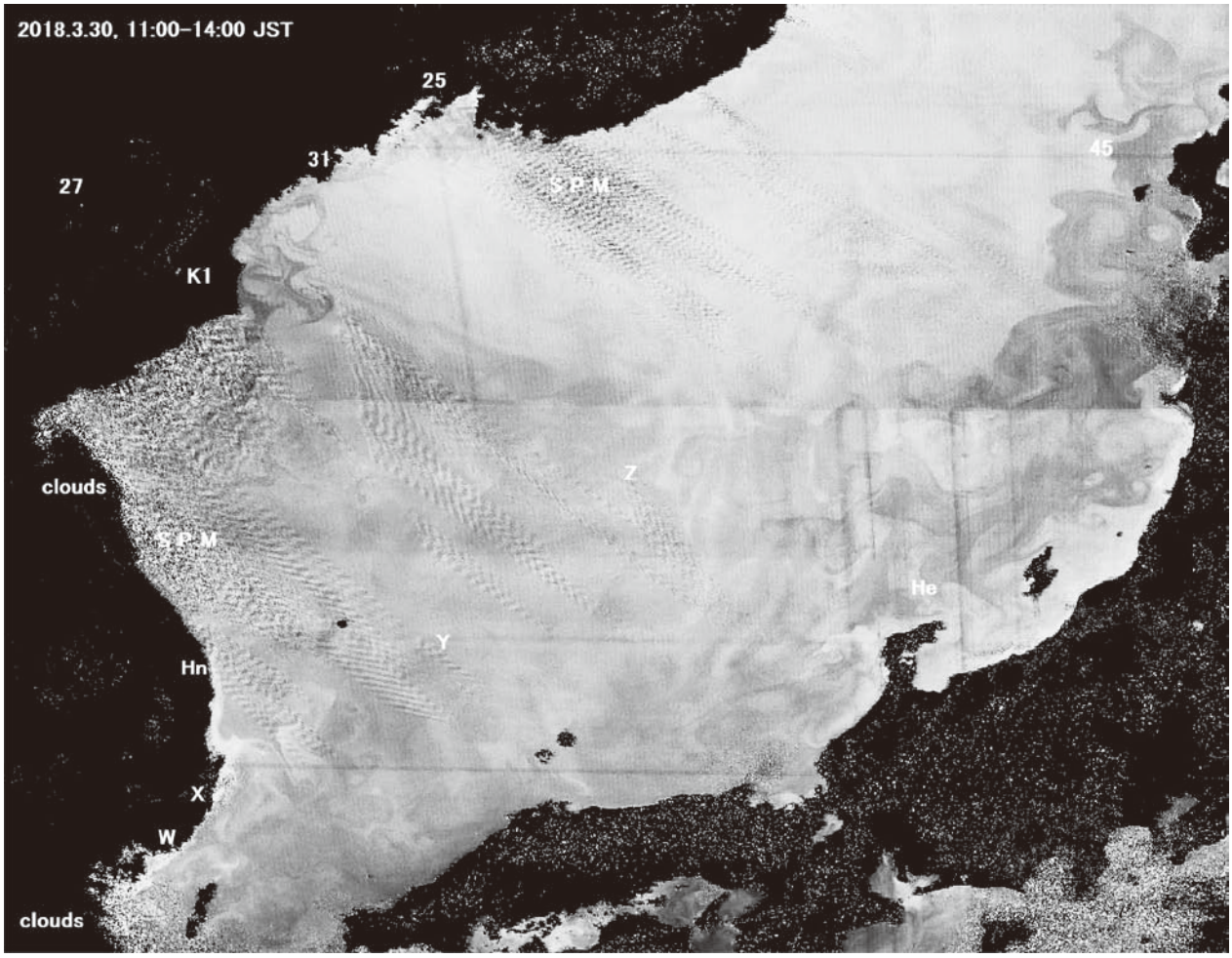


**Figure 4. The Japan Sea at 11:00~14:00, March 30, 2018.**

**Table 1. GPS for Figure 4.**

| mark | Place | E | N | Mark | Place | E | N |
|---|---|---|---|---|---|---|---|
| 23, K1 | Punggyeri | 129.0869 | 41.27833 | 31 | Russia bound. | 130.6986 | 42.29362 |
| 24 | Pyeongyang | 125.7538 | 39.03186 | 32 | Keerin city | 126.5667 | 43.86667 |
| 25 | Vladivostok | 131.9167 | 43.11667 | 33, Z | YamatoTai(S) | 134 | 39 |
| 26, S2 | Dandong | 124.383 | 40.11667 | 34, He | Hekura-jima | 136.9186 | 37.85139 |
| 27 | Changbaishan | 128.0562 | 42.0051 | 35, K2 | Nyeongbyeon NSC | 125.7621 | 39.78866 |
| 28, S1 | Sup'ung dam | 124.9625 | 40.46194 | 36, K3 | River term of NSC | 125.3679 | 39.52168 |
| 29, Y | Take shima | 131.8667 | 37.24167 | 37, X | Wolseong NPP | 129.4757 | 35.71347 |
| 30, Hn | Uljin NPP | 129.4266 | 37.05827 | 45 | **1993/7/12, M7.8 | 139.18 | 42.78167 |
| W | Pusan | 129.0333 | 35.1 | | | | |
| Se | Seoul | 126.9667 | 37.56667 | | | | |

NPP: Nuclear Power Plant, NSC: Nuclear scientific Research Center, **epicenter

(3) There is a black belt that goes from the Korean Peninsula to Japan through Yamato sedimentary (Z). It means substances flows. Darkness of the belt increases near Japan coast. We believe the phenomenon is changes of compounds (organic matters changing to corrosive acid). It is necessary to sample and analysis seawater.

(4) Substances (dark matter) flow into the Japan Sea from coast near Punggyeri (K1 point).

(5) The sea is eutrophicated nearby two Korea nuclear power plants (NPP) (Hn and X points).

Satellite images show relative distribution of substances currently. (1) To infer the meaning of the figure; (2) To

infer the relation with accidents and events happened in the past; we will withhold them. But; the following description in Wikipedia Japanese version [6]; it suggests that pollution in the Japan Sea is progressing in the long term gradually. Although it is not an academic description, we translate/describe them here.

1. Sea plants in coastal areas die and entire rocks appear. The phenomenon is seen like as whitey burning over, which is called "iso-yake". Now, it is observed throughout coasts of the Japan Sea.

2. It is considered to be caused by a change seawater. Because it is less in places near rivers where water flows in.

3. Today, "iso-yake" is familiar seeing; however, half a century ago, the coastal areas had full seaweeds, which rocks were rarely seen under them.

Radioactive Cesium is detected as following [7];

$^{137}$Cs concentration in June 2011 is 1.5~2.8 [mBq/L] that is 1~2 times higher than that of before the accident. The northeastern and southwestern parts are 2.2~2.8 and ~1.5 [mBq/L]. It shows a moving function for substances in Tsushima current.

We make an image for the southern part of the Japan Sea. The season is the summer when many kinds of planktons are activated.

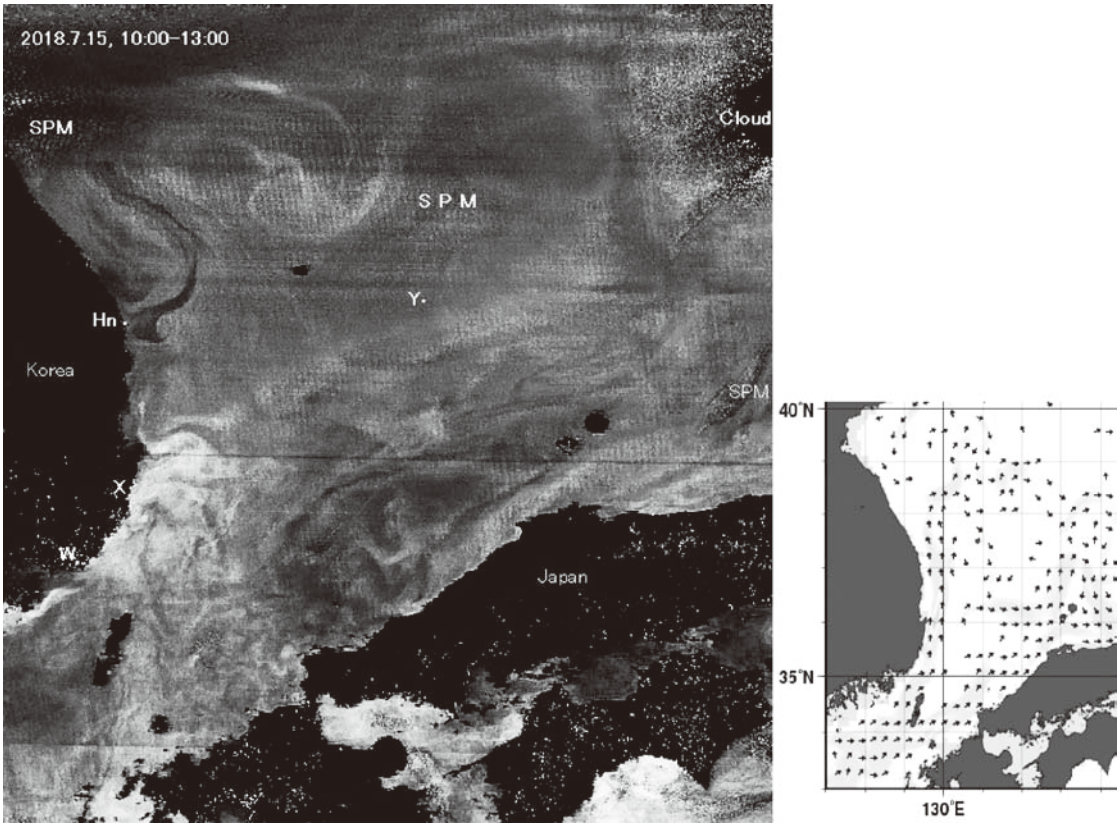


**Figure 5. Summer of the southern part of the Japan Sea at 10:00~13:00, July 15, 2018.**

The figure includes clouds, SPM, sea surfaces, and undeleted scan lines. Clouds are black (using section 3.1; {thR,thG,thB}={59,93,110}). The SPM patterns are vertical stripes by section 3.2. "N" of Eq.(5B) is 73, and "f"-factor of section 2.2 is 0.5, and "a,b" of section 2.4 is "14, {-640,0,-90}". The eye-power is ~8.5 times stronger than human. An ocean current map attached on the right side is for 11 o'clock on the same day, drawn by the observatory [5,9]. A lot of vortices and dark stream exhausted from Uljin NPP are detected. The black flow rotates to the right, and it eutrophies the sea. So, it is a rich stream of nutrients salts. The sea around Wolseong NPP is eutrophicated. The density of radioactive substances is not detected in the image, which must be measured by sampling of the sea water. The image gives the points to be sampled.

### 5.2 East China Sea

On January 6, 2018; a tanker Sanchi and cargo ship CF-Crystal collision occurred. We report the accident and the subsequent marine pollutions [8]. At that time, we point out that pollution in the East China Sea is serious. This section examines the contamination in detail.

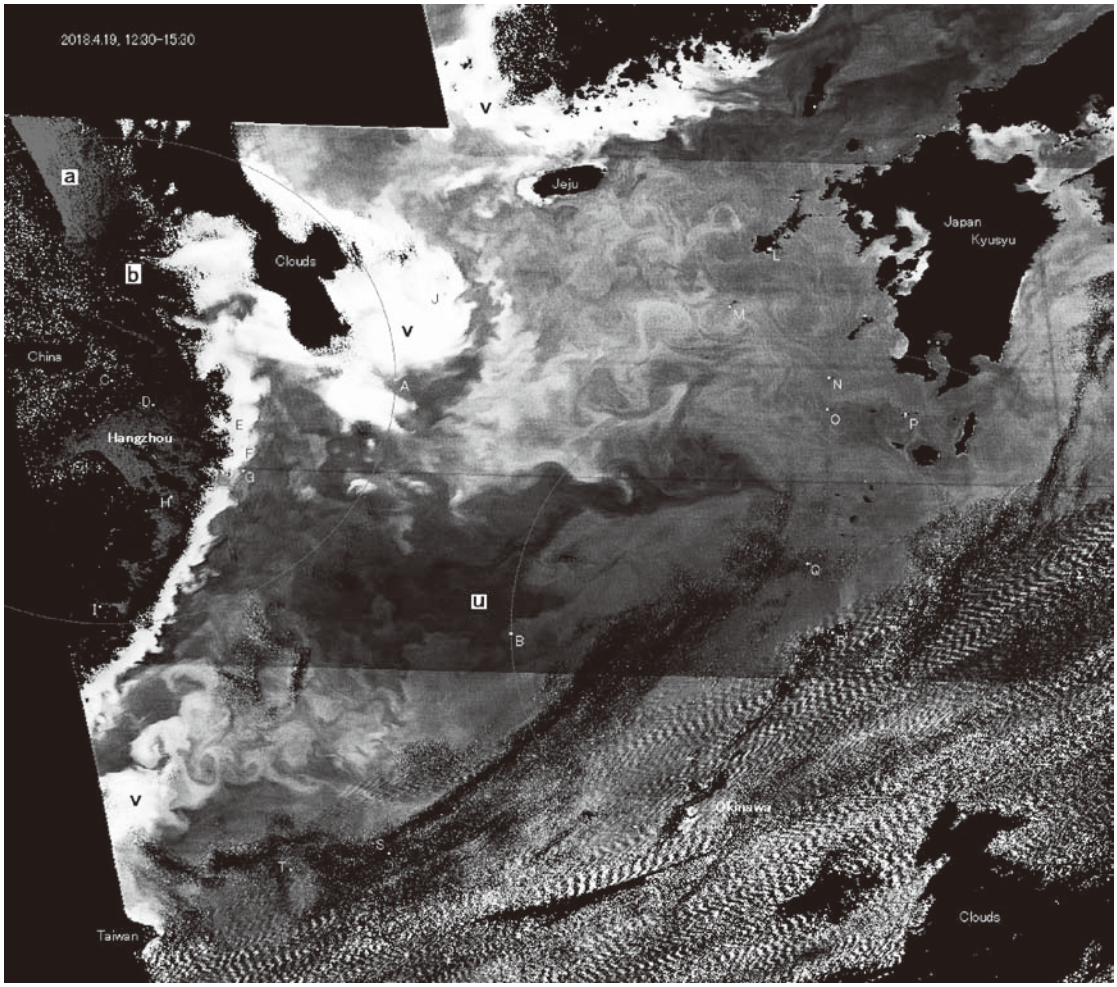


**Figure 6. The East China Sea at 12:30~15:30, April 19, 2018.**

**Table 2. GPS of Figure 6.**

| mark | point name | E deg | N deg |
|---|---|---|---|
| B | Sanchi sink point | 125.9167 | 28.3667 |
| A | Shanghai E 300km | Accident | Point |
| C | Shanghai center | 121.4833 | 31.1667 |
| D | Circle, Shanghai SE | 121.9403 | 30.8983 |
| H | other side of point D | 122.1439 | 29.8853 |
| E | Shenngsi Islands | 122.8176 | 30.7220 |
| F | Langgang Mt. Is. | 122.9336 | 30.4376 |
| G | Zhōushān Islands | 122.9446 | 30.1718 |
| I | Taizhou city | 121.35 | 28.6667 |
| J | Socotra Rock | 125.1824 | 32.1230 |

| mark | point name | E deg | N deg |
|---|---|---|---|
| L | Gotoh(Fukue) | 128.8408 | 32.6956 |
| M | Danjyo islands | 128.3519 | 31.9889 |
| N | Uji islands | 129.4503 | 31.1963 |
| O | Kusagaki islands | 129.4325 | 30.8467 |
| P | Satsuma Ioujima | 130.3053 | 30.7931 |
| Q | Takara Jima | 129.2083 | 29.1458 |
| R | Amami city | 129.4938 | 28.3772 |
| S | Taisyou Jima | 124.56 | 25.9225 |
| T | Uotsuri Tou | 123.4714 | 25.7425 |

The figure includes clouds, SPM, sea surfaces, and undeleted scan lines. Clouds are black (using section 3.1; {thR,thG,thB}={54,85,100}). The SPM patterns are vertical stripes by section 3.2. “N” of Eq.(5B) is 49, and “f”-factor of section 2.2 is 0.5, and “a,b” of section 2.4 is “10, {-400,0,0}”. The eye-power is ~7 times stronger than human.

The bold mark {**a, b, u, v**} represents {brown, dark brown, black, green} color.

The green corresponds with the eutrophic area, which is also found along Korea and south China coasts. It is a serious problem that the area is vast in the East China Sea. Edges of the area reaches on Japan’s EEZ (Exclusive Economic Zone). There are a lot of vortices along the

edges. No Tsushima Current is detected here.

The brown and dark one are more contaminated sea than the green. Larger objects compared with planktons would drift on the sea. The black part is tanker's heavy oil or the spoilage matters of eutrophication seawater. Considering the mass, the ratio of spoilage one is bigger.

### 5.3 Boundary between Kuroshio and Oyashio

Japan Coast Guard (JCG) [10] publishes the status of Kuroshio [11] per every week. On the expressions, currents are as if they are meandering rivers, which is correct information as water's flow on the 2D plain.

We believe that the images of moving substances are not such rivers. Where many vortices are observed, and 3D flows would be arisen. Such information is derived by approaches in sections 2 and 3; *that is*, the Kuroshio of April 30, 2018 is displayed in **Figure 7**. Substances flows in the Kuroshio have hierarchical structures of various vortices. Rotations of vortices are left and right, and rising/sinking flows exist there.

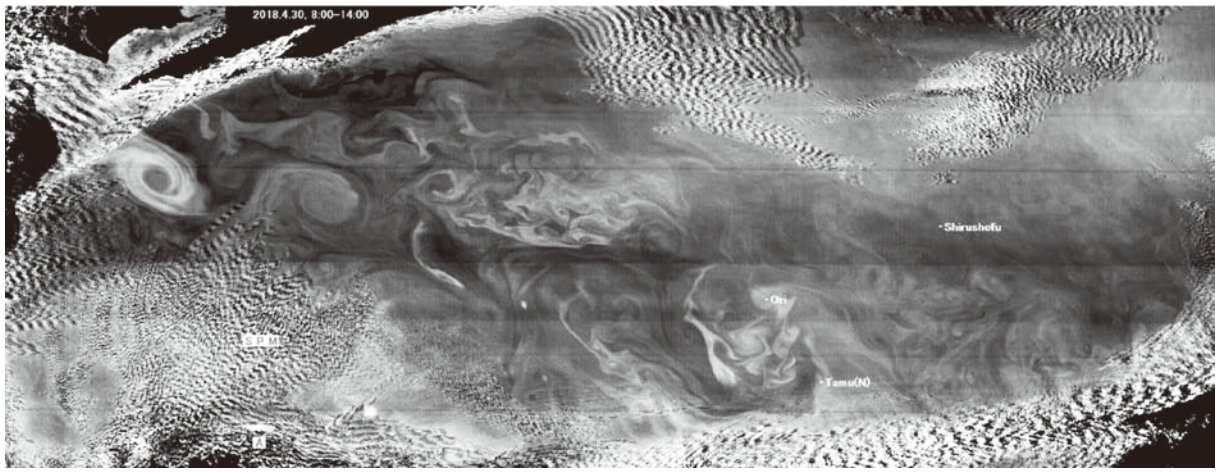


**Figure 7. Boundary zone between Kuroshio and Oyashio, at 8:00˜14:00, April 30, 2018.**

Time interval is 10 min, in which includes clouds, SPM, sea surfaces, and undeleted scan lines. Clouds are black (using section 3.1; {thR,thG,thB}={54,85,100}). The SPM is stripes by section 3.2. "N" of Eq.(5B) is 37, and "f"-factor of section 2.2 is 0.5, and "a,b" of section 2.4 is "20,{-330,20,70}". The eye-power is 6 times stronger than human. Massifs in **Figure 7** are in **Table 3**.

**Table 3. Massifs GPS.**

| Massif | E deg | N deg |
|---|---|---|
| Shirushofu | 162.5 | 38 |
| Ori | 158.3 | 36 |
| Tamu (N) | 159.5 | 34 |
| Tamu (S) | 158.5 | 32 |

Strong bluish vortices are found near A-point about 150E and 33N. Since the details are covered by clouds and SPM, we show **Figure 8** that is at April 22, 2018.

Time interval is 1h, in which includes clouds, SPM, sea surfaces, and undeleted scan lines. Clouds are black (using section 3.1; {thR,thG,thB}={59,93,110}). The SPM is stripes by section 3.2. "N" of Eq.(5B) is 8, and "f"-factor of section 2.2 is 0.5, and "a,b" of section 2.4 is "12,{-180,0,-70}". The eye-power is ~3 times stronger than human.

There is no vortex at a point (148E, 33N) in JMA current map of the day [9]. The diameter is about 30km on the pixel numbers. It is left-rotating; thus, the vortex aspirates seawater. As a circumstantial evidence; there are bright plankton belts grown in the deep nutrients aspirated around the vortex.

Such a blueish vortex is reported by NASA's satellite "Terra", which event is found at 10:11, February 23, 2011, where the location was at south of the Africa continent. The Japanese commentary "BuzZap" writes that the blue 150km vortex is not an abnormal phenomenon, but pumps up nutrients from deep sea floor to a sea surface and enriches the ecosystem [12]. The counter-clockwise vortex is thought to have peeled off from the Agulhas Current, which flows along the southeastern coast of Africa and around the tip of South Africa [13].

Here; we show a structured vortices offshore Japan east.

Time interval is 2.5 min, in which includes clouds, SPM, sea surfaces, and undeleted scan lines. Clouds are

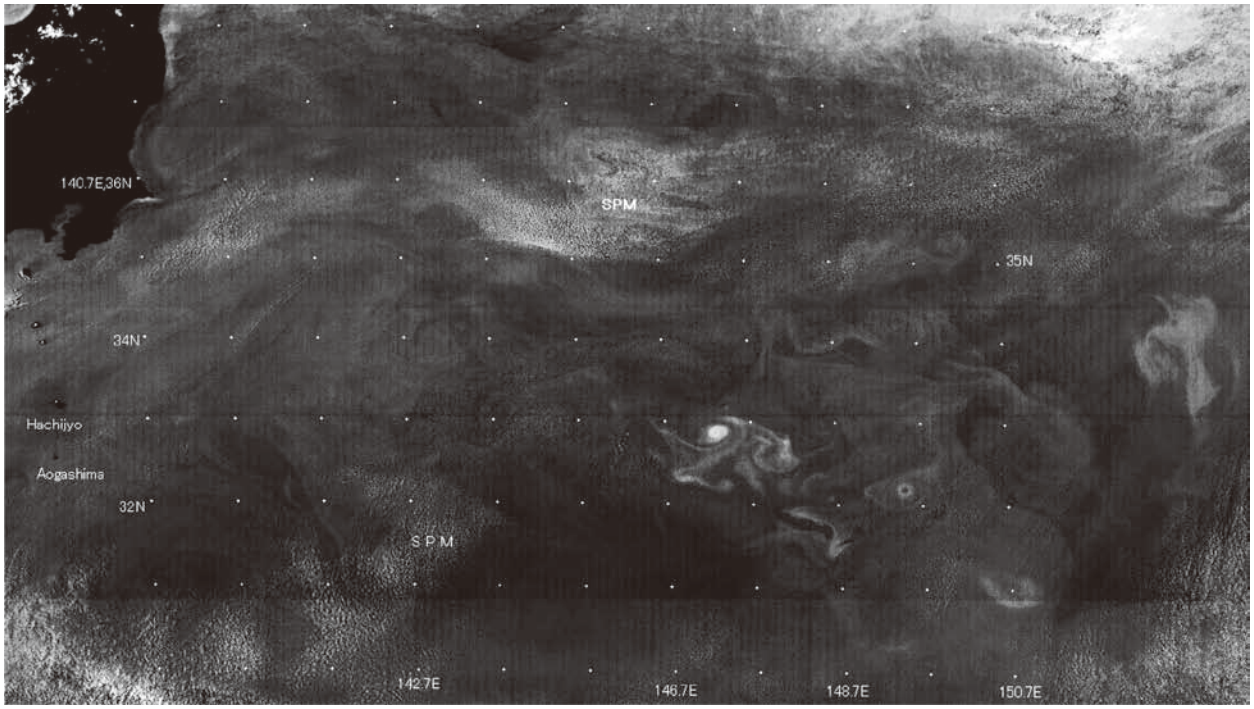


**Figure 8. Vortices in the Kuroshio at 8:00˜15:00, April 22, 2018.**

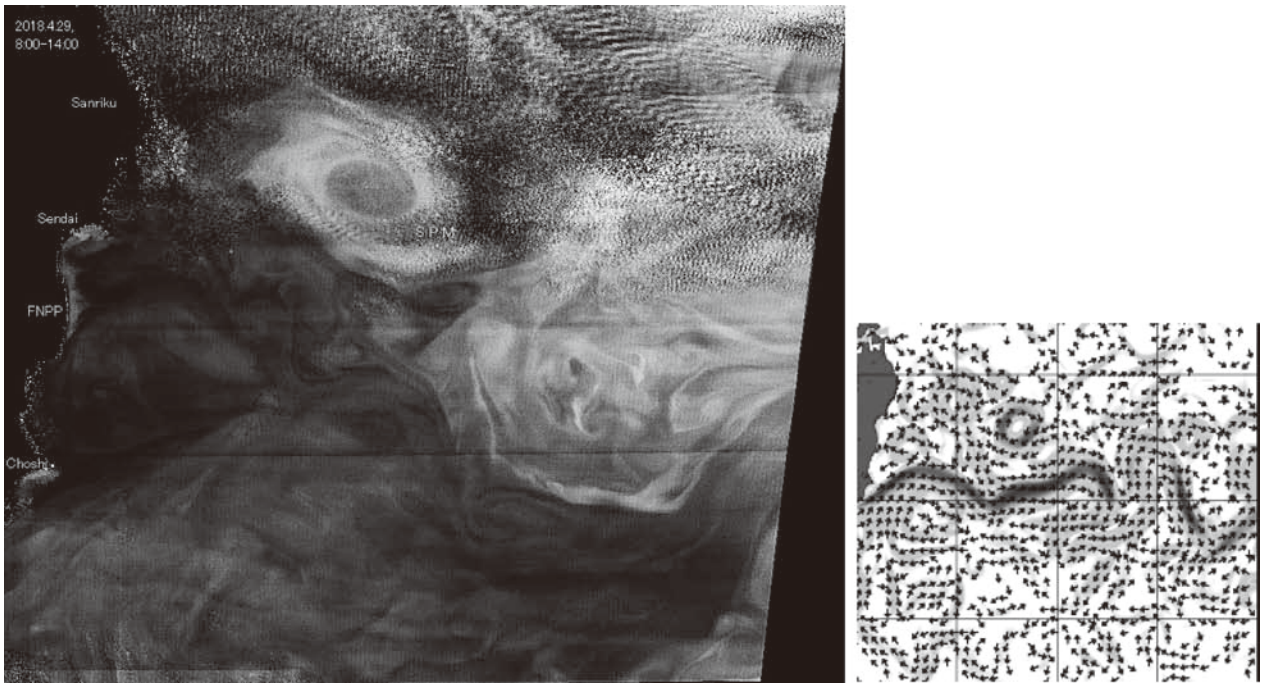


**Figure 9. Vortices offshore Japan east, 8:00-14:00, April 29, 2018; and daily 50m currents [9].**

black (using section 3.1; {thR,thG,thB}={49,76,90}). The SPM is stripes by section 3.2. "N" of Eq.(5B) is 145, and "f"-factor of section 2.2 is 0.5, and "a,b" of section 2.4 is "20,{-900,0,-150}". The eye-power is 12 times stronger than human.

In **Figure 9**, it is clear substances/water currents are different. A simple convection-diffusion equation would not give the substance distribution based on the sea current field. The upper-left vortex has right-rotating character, thus, it is a sinking function.

It is surprising that remarkable vortices as shown in **Figure 7~9** are found in the far offshore Pacific Ocean from Aogashima to Sanriku. There is no seamount near the vortices, and the cause is unknown. It is an important

to research the results for vertical flows of the vortices. We believe that detecting movements of substances, the distribution of radioactive Cesium (Cs) is effective index. There are 4 references about accidents of Fukushima 1st nuclear power plant [14~17]. Their abstracts are followings;

(1) Cs concentration in the surface layer is about 10~100 [mBq/L] initially. It diffuses on northern side of Kuroshio until the central area of North Pacific Ocean during 6 months.

(2) On the Ocean's central area, Kuroshio slows down, and the diffusion for north/south-directions is promoted. The Cs concentration becomes rapidly lower by the wide extensions.

(3) On the south side of Kuroshio continuous flow, the Cs is taken into the water mass called "mode water" instead of the surface layer, and it becomes clear that the Cs is transported to interior of the Ocean.

(4) Since the Cs in the mode water is transported to the west, opposite direction against the surface layer. It is confirmed in waters at south of Japan. The mass ratio is ~10%.

### 5.4 Blue tide offshore Midway

#### 5.4.1 Outlines

The phenomenon is seen like as a blue tide. It is found from June to August on the sea surface from the Shatsky-rise to the North of Midway, where Kuroshio is weakening. We detect it every year from 2016. The period in 2018 is from June 1 to August 26. It is moving, and new one is appeared at west side rarely.

The blue tide in Japan is often found inner the bay. The cause is colloidal sulfur particles. The red tide is occurred by planktons; the color is not only red but also sometimes blue.

On a general theory, it is enough that plankton will occur in upward flows [18,19]. For example, Hurricane Isabel stirs Atlantic Ocean water in Sep. 13~18, 2003, the blue tide is found [20]. The scale is about 500km that equals to the Florida Peninsula. Midway's blue tide is about 1900 km at 2017, which has many vortices and complex structures. The image has many noises after erasing clouds; therefore, it is hard to see blue tide in monochrome. It is not posted. If you need it; would you please request it to authors (until July 2019) or access to Appendix in Web-version.

The existence of fine structure is a different point from Hurricane Isabel's case. The vortices have both directions of rotation.

#### 5.4.2 Getting detail images in 2016

The reference sea is covered by many clouds and mists during the season. A part of the phenomenon can be seen among storm-clouds. The imaging is difficult; therefore, even if approaches of section 3.1 and Eq.(5B) are used, some clouds and many SPM are remained. The time of accumulated original images are non-equivalent intervals, *i.e.*;

6 images: 8:00~10:00, per 1 h, at May 28 and 31, 2016;

24 images: 7:30~10:00, per 30 min, at May 29, 30, June 1, 2, 2016.

In case of such intervals, Eq.(5D) is inappropriate.

An example is **Figure 10**. Where; you must interpret the phenomenon, and recognize partial vortex-like patterns. Parameters of section 3.1 are {thR,thG,thB}={54,85,100}. And "f"-factor of section 2.2 is 0.5, and "a,b" of section 2.4 is "12,{-80,-30,0}". The digital gradation filter is adopted.

If coloring is allowed, since SPM is green, the phenomenon is separated clear. The GPS points, J~Q, is in **Table 4**. There are patterns found from NW to SE directions around the S-point; they are 3 bluish vortices (in case of printing they are white ones). We recognize them as the phenomenon.

#### 5.4.3 Causality and discussion

Why the phenomenon is appeared? The blue tide is phenomenon that sulfur contained in sea water becomes colloid and seawater becomes cloudy, and is seen as light blue. White tide [21] is known also, which is a kind of the red tide, relates with outbreak of planktons, Eucampia Zoodiacus. Both of them are mixed effects among sea surface and lower layers. And macronutrients must be supplied there, which is not a point but broad area about 2000 km. Does such a condition hold offshore Midway? Mass supplier for extensive waters is insufficient by one typhoon or low pressure.

"Thermohaline Circulation" in Japanese Wikipedia [22] explains "Since the deep water has chemical characteristics due to substances sinking and decomposing; by searching for it in surface layer of North Pacific Ocean, you may detect where a large upward flow occurs".

There is a spring point at the center of North Pacific Ocean, in which is in the Great Ocean Conveyor Belt (GOCB) [23]. However; since the point is from the deep sea to a mid-layer, as the surface, the information is uncertain.

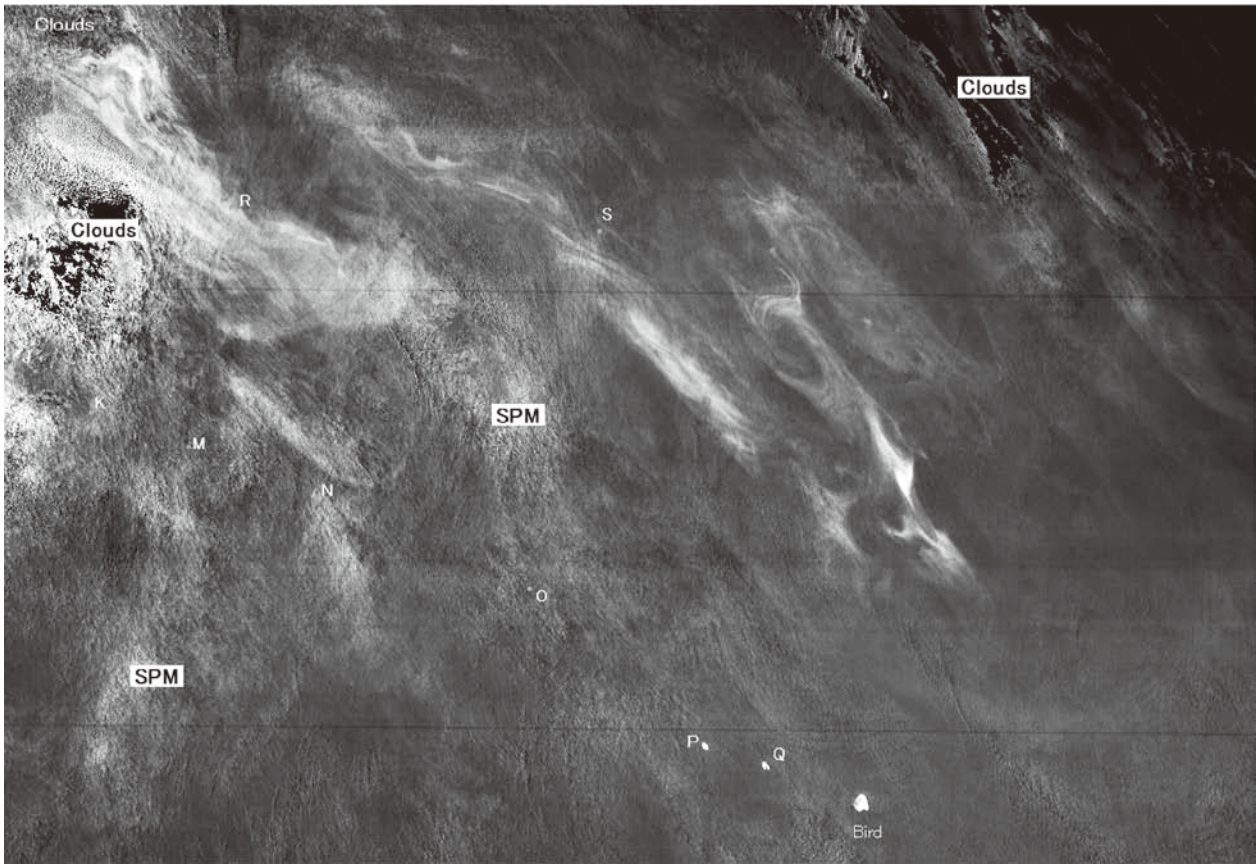


**Figure 10. Blue tide offshore Midway from May 28 to June 2, 2016.**

**Table 4. GPS points for Figure 10.**

| mark | point name | E deg | N deg |
|---|---|---|---|
| J | Yuryaku | 172.27 | 32.67 |
| K | Kanmu | 173 | 32.167 |
| L | Daikakuji | 172.3 | 32.08333 |
| M | Abbott | 174.3 | 31.8 |
| N | Colahan | 176 | 31.25 |

| mark | point name | E deg | N deg |
|---|---|---|---|
| O | Hancock | 178.833 | 30.25 |
| P | Kure island | 181.6849 | 28.39889 |
| Q | Midway island | 182.6312 | 28.23233 |
| R | Setting pt.1 on 35N | 175 | 35 |
| S | Setting pt.2 on 35N | 180 | 35 |

We believe in a JAMSTEC (Japan Agency for Marine-earth Science and Technology) simulation "10 km resolution half-global ocean long-term past reproduction experiment [24]". The paper concludes "Influence of bomb cyclone (strong low pressure in winter; called winter typhoon also) on the ocean". It explains that a strong upward flow from vicinity of seabed is excited under the divergent area of the cyclone. The excited vertical flow maintains about 1 week as inertial vibration. Horizontal divergence is excited in the ocean mixed layer from surface layer to 60 m, and upwelling flow of the low pressure scale is formed up to around 2 km below. In the deeper layers there is an upwelling along seafloor topography such as seamount.

Those knowledges are fragments and circumstantial evidences; there is no research connecting them directly.

#### 5.4.4 Importance of GOCB

GOCB is related to the global warming. Heat generated by human civilization warms atmosphere and ocean. The heat capacity is overwhelmingly larger in ocean [25]. We believe the oceanic heat circulation determines the future of global warming. The thermal circulation including deep layers is being investigated; that is, GOCB.

One cycle of GOCB is believed about 1200 years. There is a sinking point of GOCB, which locates in the Norwegian Sea. (Based on ref.[26], there are 3 points; Weddell Sea, Ross Sea, and Norwegian Sea.)

If the beginning of global warming is assumed to be 1950, it gives no influence until 3150? It will not come out

at least the ocean depend part, if earth environment is fixed. But, what happens, if the speed changes, or GOCB pipeline is cut off, and is branched?

Dr. Hasumi points out that there is less source of generation/disappearance of heat and salt in interior of the ocean. The cause of characteristic densities as the temperature and salinity in sea water is on surfaces only. The sea water existing in the ocean is exposed to the surface at past stage, if it follows the circulation [26].

Influence of GOCB stream change is easy to detect near fountain points from deep layers. However, it locates in mid layers, does not exist on the surfaces. We must monitor the special surfaces where there is the rising flow up from the mid layers. Such conditions are held on the sea surfaces around Midway island.

Pause phenomenon of the global warming has occurred since about 2000. It is called the hiatus. The cause is simulated, and it is "Pacific decadal scale fluctuation". The period is supposed to be about 15 years. Therefore now, it is meaningful to search surfaces on the Pacific Ocean [27].

### 5.5 Convection-Diffusion in Atmosphere

Photographically viewing the convection-diffusion of small particles in air, the convection part is detected easily. Getting images of the diffusion is a rare case in natural. In the atmosphere of excess moisture, the particles gather water in chain reactions around SPM particles as catalyst. In a before step cloud formations, the image like diffusion may be detected. The moisture adsorption reaction is a competition with the inverse transpiration. Therefore, an image of the stage becomes a complicated shape related with humidity distribution.

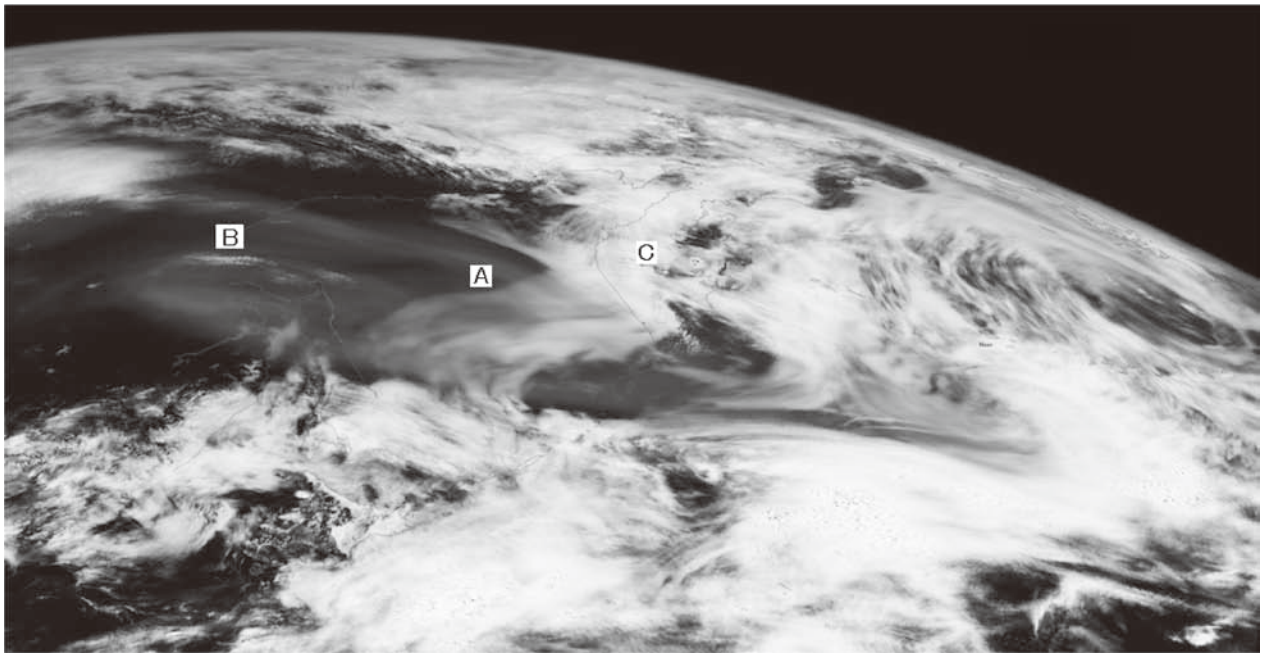


**Figure 11. Black mist on the Okhotsk Sea.**

This is got at 8:00~10:10 (per 10 min), August 12, 2015. N in section 3.2 is 14, and {thR,thG,thB} in section 3.1 is {119,187,220}. "f"-factor of section 2.2 is 0.0, and "a,b" of section 2.4 is "1,{50,0,0}". Wave length dependency is n=-1.5 in section 3.1. The picture's power is equal to the human.

Marks A, B, C are the black mist, small clouds row, and clouds on Kamchatka Peninsula. Sakhalin is found slightly under the mist. Comparing A and C, it understands there is the black mist on the clouds. We observed such a diverged mist at 2.8 km point in Mt. Norikura [28].

We need to pay attention to Mark B's surrounding atmosphere, and processing there, we get **Figure 12**. It is a strong westerly wind around B-point, and the chain reaction point moves to the east. Complex patterns under the B-point show time series of the reaction. Such a reaction of formation/annihilation between vapor and clouds in air including SPM is detected even at altitude of several hundred meters [29].

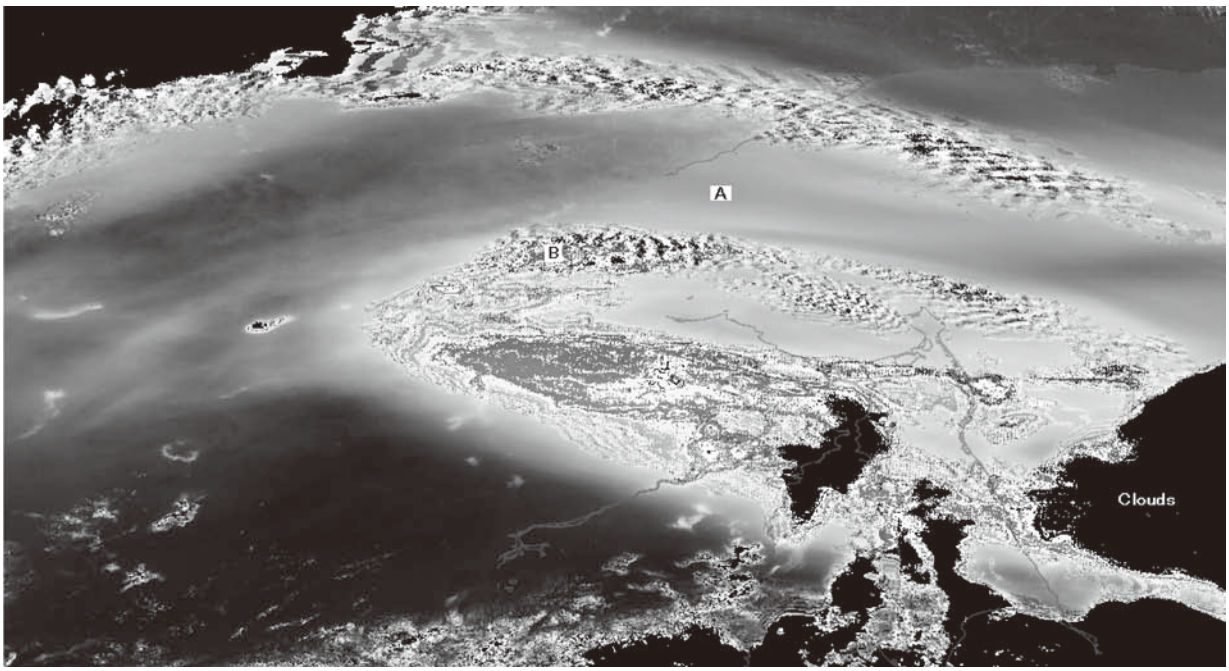


**Figure 11. Black mist on the Okhotsk Sea.**

Marks A and B are the black mist and small clouds. Complex patterns under mark-B are convection-diffusion phenomena that are drawn by Eq.(5D). The stripe interval is per 10 min.

## 6. Multi spectra Analysis

### 6.1 Libra-Data Base

Objects in images are reflectance patterns. Satellite images have an advantage that target range is vast. It is difficult to do by using conventional measurements. However; it is necessary to verify the correspondence between reflectance and substance concentration at several points in the image. It is a missing part in previous sections. Then, using Chlorophyll-a (Chl) and Suspended Solids (SS) indexes, the environmental characters at target-points are investigated.

We go to "Libra-data base". The Libra is a browser for open Landsat 8 satellite imagery [30]. You can use it to browse, filter, sort, and download images [31]. It is collaboration between the National Aeronautics and Space Administration (NASA) and the United States Geological Survey (USGS). Landsat-8 has following specifications (*cf.* **Table 5**): the perigee, apogee, inclination, period are 701.0, 703.0 km, 98.2248 deg, 98.8 min. Each image is 180 × 180 km, and about 7800 × 7800 pixels. The image format is Tif16, ~60 MB/1-image.

**Table 5. Specifications of Landsat-8.**

| Band | characters | Wavelength (wL) | Resolution | Solar Irradiance* |
|---|---|---|---|---|
| Band 1 | Coastal/Aerosol | 0.433 - 0.453 μm | 30 m | 2031 W/(m²μm) |
| Band 2 | Blue | 0.450 - 0.515 μm | 30 m | 1925 W/(m²μm) |
| Band 3 | Green | 0.525 - 0.600 μm | 30 m | 1826 W/(m²μm) |
| Band 4 | Red | 0.630 - 0.680 μm | 30 m | 1574 W/(m²μm) |
| Band 5 | Near Infrared | 0.845 - 0.885 μm | 30 m | 955 W/(m²μm) |
| Band 6 | Short Wave Inf.1 | 1.560 - 1.660 μm | 30 m | 242 W/(m²μm) |
| Band 7 | Short Wave Inf.2 | 2.100 - 2.300 μm | 30 m | 82.5 W/(m²μm) |
| Band 8 | Panchromatic | 0.500 - 0.680 μm | 15 m | 1739 W/(m²μm) |
| Band 9 | Cirrus | 1.360 - 1.390 μm | 30 m | 361 W/(m²μm) |
| Band 10 | Long Wave Inf.1 | 10.30 - 11.30 μm | 100 m | |
| Band 11 | Long Wave Inf.2 | 11.50 - 12.50 μm | 100 m | |

* The wavelength dependency is,

$wL^{-0.81}$($R^2$=0.998, 0.44<wL<2.2 μm), *or*

$wL^{-0.50}$($R^2$=0.97, 0.44<wL<0.66 μm). (7)

Thus, an equivalent RGB-synthesis gives a bluish image. The image size is too large to process them in 32-bits OS (ex. Windows-7 personal, 4 GB). We adopt following file conversions. Using the Windows-paint, convert Tif16 to Gif. On the processing, make downsizing of 1/4. The output file size is about 1 MB and 2000×2000 pixels; any processing is enable. The 1/2 of dynamic range information is cut off during the conversions. If you can use 64-bits OS and large memory, you should process in Tif16.

### 6.2 Aspects near the Zhōushān Islands, Dàishān district in China

We make attention to Chlorophyll-a (Chl) and Suspended Solids (SS) for status of the water, and do to normalized difference vegetation index (NDVI) for the ground. The definitions are;

Chl(ij)=Bij/Gij, (8A)

SS(ij)=Rij/(Rij+Gij+Bij), (8B)

NDVI(ij)=(IRij-Rij)/(IRij+Rij), (8C)

When the denominator is small value (ex. <10), each index is set 0. The expression is derived from refs.[32,33].

The order is “from the top left to right; one step down, left, then right”. The date is July 19, 2018, when the cloud ratio is 6.90%, and the angle of the Sun is 108.13 deg. Each image is 82.12×76.47 km for horizontal and vertical

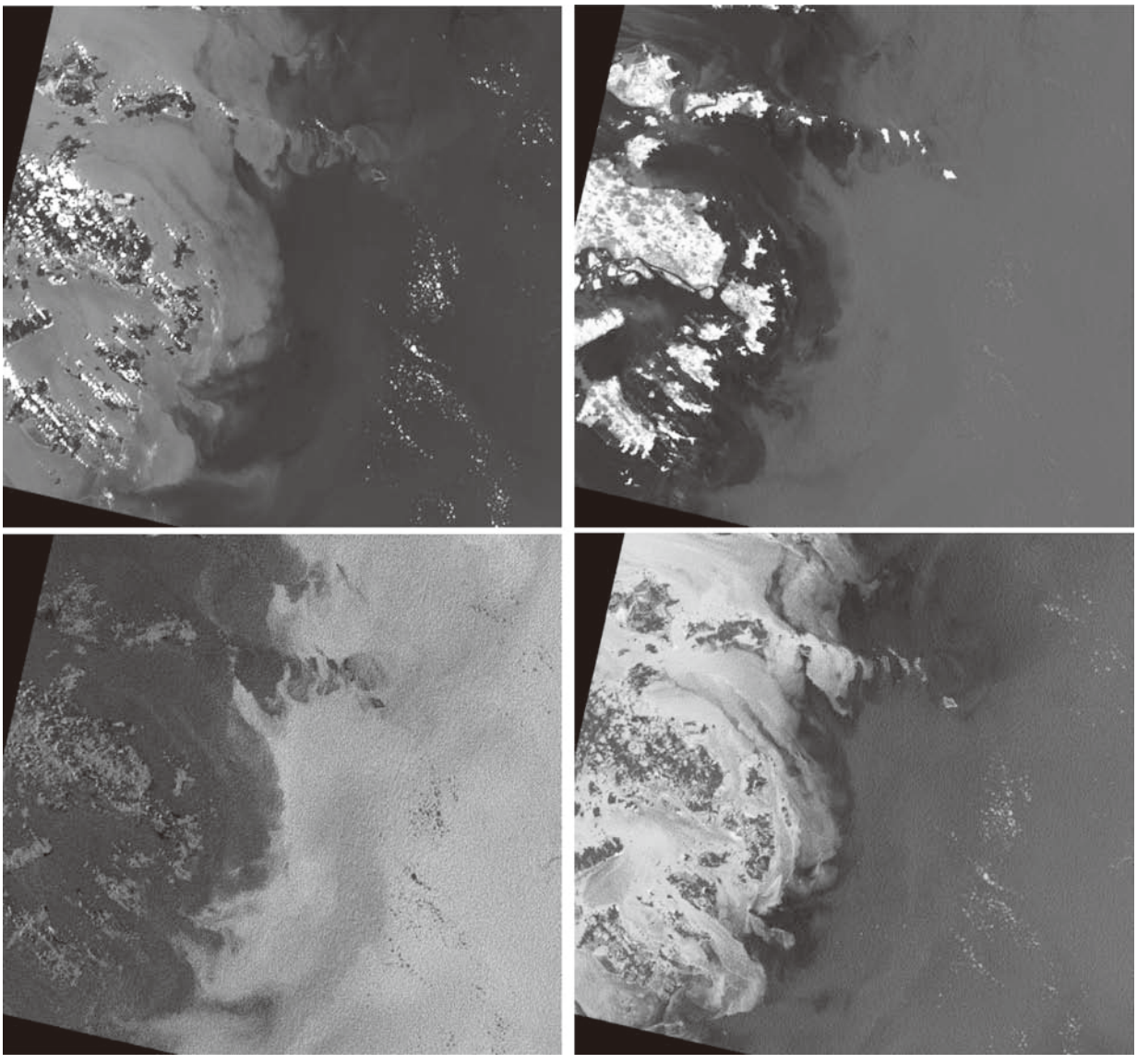

**Figure 13. Monochrome-, NDVI-, Chlorophyll-, and SS-images near the Zhōushān Islands (Dàishān district in China).**

directions. Amplifiers of the images are 3, 2, 3, 3 times, respectively.

We interpret the images that; (1) white clouds are detected by the monochrome, and the locations of islands are corresponded with an internet map (ex. Google Map).
(2) NDVI image gives information for vegetation on the ground, but doesn't do distribution of the green algae. A strong absorption effect is in red and infrared bands, which is the property of the water. Eq.(8C) in the water gives less information. Lagoon around small islands is processed darkly; because of large amount of SS emits red light.
(3) Chlorophyll image indicates the distribution of plants plankton's Chlorophyll-a. It is negative patterns by Eq.(8A). It is got by absorption of the blue light.
(4) SS image is got from Eq.(8B), which equals to normalized Rij. The strong patterns are in lagoons among small islands, and they seem to be like mud streams. In out zone around the SS patterns, a weak black Chlorophyll-a stream is found and it is diffused towards the north. Those phenomena are arisen nearby the point-G in **Figure 6** (section 5.2).

### 6.3 Status around Wolseong NPP in Korea

We point out that the sea around Wolseong NPP is eutrophicated in section 5.1. The cause is considered to be seawater warming. To detect the phenomenon, the most appropriate spectrum band is in the thermal infrared. **Figure 14** is the band image.

The figure size is 72.656×56.250 km. The date is July 14, 2018, where the cloud ratio is 2.27%, and the sun angle is 120.01 deg. Mark-A is the warmed sea water area. A warmed area is spreading to the north while bending to the left. To interpret the figure, a visual image is also necessary.

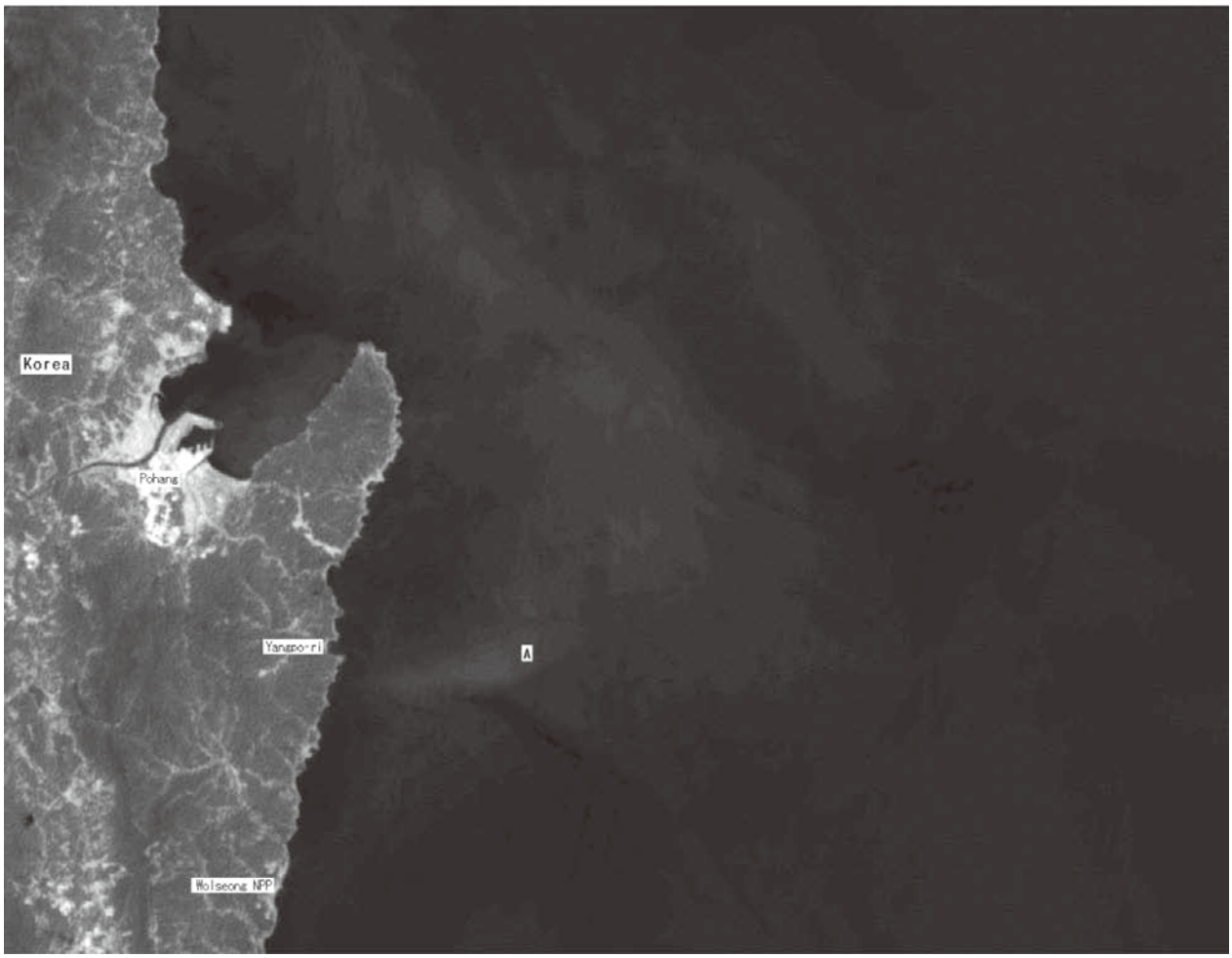


**Figure 14. Band-10 (10.30~11.30 μm) image near Wolseong NPP.**

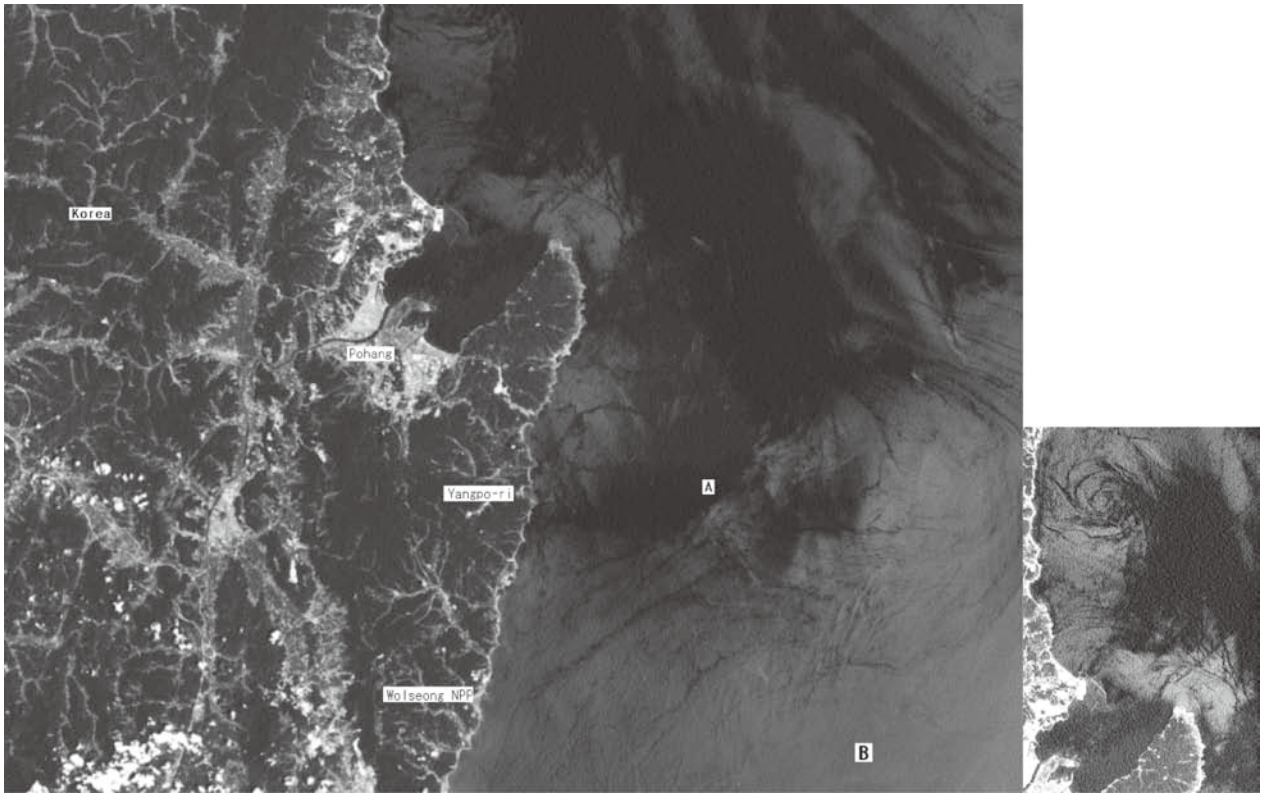


**Figure 15. A monochrome image converted from RGB (0.45~0.68 μm), near Wolseong NPP and the north direction from Pohang city.**

The figure is amplified by 8 times, whose area and date are same as that of **Figure 14**. Mark-A, B are the warm sea water and white surfaces. The right small image is a clack part as if it seems to be a vortex.

We think the white part is thin films or bubbles. It is not gas/liquid phase; because of many clack patterns are found on the B-area, and a rotation pattern is also. The whiteness is in **Figure 16**, where B/G ad G/R ratios are plotted.

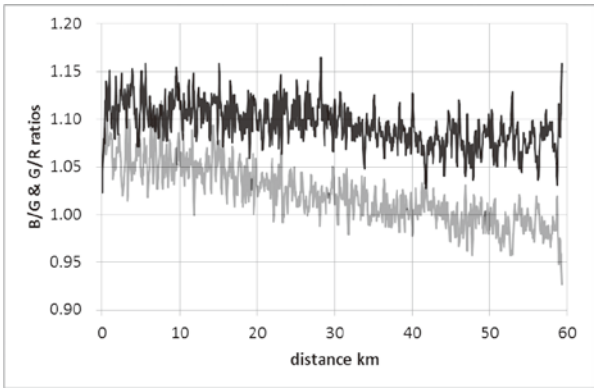


**Figure 16. B/G and G/R ratios of the whiteness degrees.**

Horizontal axis is the distance [km] from Wolseong NPP. The direction is towards the East strightly. Vertical axis is ratios. Upper zigzag line is B/G-ratio, and another is G/R. The calculation is done by using Eq.(7).

The B/R-ratio is between 1.15 and 1.05; therefore, absorption band of the Chlorophyll-a is not detected. The B/R-ratio downs gradually, its vales are from 1.05 to 0.95. Thus, the hue is pale bluish white.

There is the Kori NPP that is the south 46.9km from the Wolseong NPP. As comments near the Kori NPP (they are in internet [34]), (1) A sea lady who works near NPP says “When white bubbles float in sea, water gets bitter”. (2) The NPP exhausts dimethylpolysiloxane 100t, which is mixed into the drainage; the period is from January, 2011 to August 2016. The compound reduces the surface tension, and makes antifoam actions. When draining water used to lower the temperature of NPP to the sea, a lot of foam is generated.

This information was in internet: Wolseong NPP exhausts $^{3}$HOH 3.63t in the primary coolants. The clock is 18:44, June 11 in 2018.

This is the limit of photographic approaches. Next is chemical analyzing them, it is necessary to take seawaters.

Warm water at Mark-A is found at clacks of the white films. Existence of the warm water is uncertain under the

films. Thus, it is necessary to investigate compositions of sea water in the area.

## 7. Conclusions

To extract environmental information from satellite pictures, computer approaches are proposed. One is for visual spectrum bands, which can be applied to images of commercial digital cameras. Using them, we can see invisible phenomena in the sea or atmosphere. Another is for multi-spectra bands, which apply to research the property.

Applying those techniques, we indicate followings;

(1) We show aspects of the Japan Sea, the East China Sea, and Kuroshio in the Pacific Ocean. Meso-scale vortices and phenomenon like blue tide are displayed, and discussed. Substances flows in the Seas are appeared, which is not that of thermal-flux. The flows connect with fishery tightly.

(2) Discussions of the Kuroshio may be separated at 150E. The west area relates $^{137}$Cs sinking to mid layers in the Pacific Ocean. Cs does not penetrate through mean water column; the process would relate with vortices. The east area relates with the GOCB, *i.e.*, climate changes.
Since they are guesses from images, the re-examination of seawaters is required.

(3) We analyze pollution in the East China Sea ahead of Hangzhou Bay with multi-spectra. And we consider the status of sea surface around Wolseong NPP in Korea.

(4) We detect the convection-diffusion phenomenon in air. It relates with chain reactions around SPM in the atmosphere. The visualization would be first.

The information is an important fragment to understand the global climate changes and sea pollutions; hereafter, continuous watching is necessary.

**Acknowledgement:**

We quote the WSDBank* Web developed by NICT** science cloud.

*World Science Data Bank, **National Institute of Information and Communications Technology.

We are very thanks for allowance to access permission.

## References

[1] Kotaro BESSHO, et. al., “An Introduction to Himawari-8/9- Japan’s New-Generation Geostationary Meteorological Satellites”, *J. Meteorological Soc. Japan*, vol.94(2), pp.151-183 (2016). https://www.jstage.jst.go.jp/article/jmsj/94/2/94_2016-009/_article/-char/ja/. DOI, https://doi.org/10.2151/jmsj.2016-009.

[2] National Institute of Information and Communications Technology (NICT), Science Cloud, https://seg-web.nict.go.jp/wsdb_osndisk/shareDirDownload/bDw2maKV

[3] NICT, Himawari viewer page, http://himawari8.nict.go.jp/.

[4] Japan Meteorological Agency (JMA), “Ocean currents in the waters off Japan* (Monthly Overview)”, https://www.data.jma.go.jp/kaiyou/data/shindan/c_1/jpn_monthly/jpn_monthly_cur.html.
This is written by Japanese. If you go to the English page, same information is not got. Therefore; we recommend automatic translations. Anyone can understand data and figures. *) Interesting thing; the coast of China in the East China Sea is not included there. Where, the sea surface status is abnormal discolored.

[5] It is used to be Maizuru Marine Observatory; *Now*, a facility of JMA named the Marine Meteorological Observatory for the Japan Sea. There is no English web-page, Japanese page is, https://www.jma-net.go.jp/jsmarine/japansea.html. However; graphs or data can be understood. Many important data are there. *Cf.* reference [9].

[6] Wikipedia (Japanese), “Japan Sea”, https://ja.wikipedia.org/wiki/%E6%97%A5%E6%9C%AC%E6%B5%B7.
There is no description in English version; *So*, we translate main parts.

[7] M.INOUE, et.al., “Lateral variation of $^{134}$Cs and $^{137}$Cs concentrations in surface seawater in and around the Japan Sea after the Fukushima Dai-ichi Nuclear Power Plant accident”, *Journal of Environmental Radioactivity*, vol.109, pp.45-51, (2012.7), https://www.sciencedirect.com/science/article/pii/S0265931X12000082. https://doi.org/10.1016/j.jenvrad.2012.01.004.

[8] Junko KAMBE, et.al., “Development and Investigation of Marine Pollution Survey Method Using Sea Level Hue Change by Satellite Image of Visible Light”, *J.Compt. Chem.Japan*, 2018, in printing, https://www.jstage.jst.go.jp/article/jccj/advpub/0/advpub_2018-0014/_pdf/-char/ja, DOI https://doi.org/10.2477/jccj.2018-0014.

[9] JMA (Japan Meteorological Agency), “Daily 50m currents”, https://www.data.jma.go.jp/gmd/kaiyou/data/

db/kaikyo/daily/current_HQ.html.

[10] Japan Coast Guard, https://www.kaiho.mlit.go.jp/e/index_e.html.

[11] Ocean Current Forecasting, http://www1.kaiho.mlit.go.jp/KANKYO/KAIYO/qboc/2018cal/ocf/ocf201849.html.

[12] BuzZap news (in Japanese), 10:11, February 23, 2012, https://buzzap.jp/news/20120223-agulhas-eddies/.

[13] Beforeitsnews, "Satellite Captures Enormous Underwater Storm", 17:43, February 22, 2012, https://beforeitsnews.com/v3/space/2012/1800152.html.

We predict a left-handed vortex in the Southern Hemisphere generates a downward flow (but, "Beforeitnews" says upward flow!). Here is an interesting part.

**A consideration of the center of the typhoon.**

There is no cloud in the center of the typhoon; we call it "eye". The eye is surrounded by wall clouds that are convection clouds. The convection is upward direction, it generates a low pressure fields. Surround air (including air of typhoon's center) is aspirated towards the low pressure part. On the grand point of the center, there is no supply air; thus, it must be supplied from upper sky. Therefore, *there is a downward wind at the center* of the typhoon. It is a meteorological knowledge. Strictly prediction, the 3D vector analysis is required.

In web-pages of "National GeoGraphic", similar phenomena of the sea surface coloring are found;

(1) "Bluish vortices of planktons", offshore Ireland, at August 19, 2010.
https://natgeo.nikkeibp.co.jp/nng/article/news/14/3033/.

(2) "Plankton's swirl, off Patagonia, The colorful plankton art that appeared in the South Atlantic Ocean",
https://natgeo.nikkeibp.co.jp/nng/article/20141218/429177/.

[14] H. KAERIYAMA, et.al.,"Direct observation of $^{134}$Cs and $^{137}$Cs in surface seawater in the western and central North Pacific after the Fukushima Dai-ichi nuclear power plant accident", *Biogeosciences*, vol.10, 4287-4295, 2013;
https://doi.org/10.5194/bg-10-4287-2013.

[15] Hideki KAERIYAMA, et.al.," Southwest Intrusion of $^{134}$Cs and $^{137}$Cs Derived from the Fukushima Dai-ichi Nuclear Power Plant Accident in the Western North Pacific", *Environ. Sci. Technol*., 2014, vol.48 (6), pp 3120–3127; DOI: 10.1021/es403686v.

[16] Maderich V., Bezhenar R., Tateda Y., Aoyama M., Tsumune D., Jung, K. T., de With G.,
"The POSEIDON-R compartment model for the prediction of transport and fate of radionuclides in the marine environment." *MethodsX*, vol.5, pp1251-1266 (2018). https://doi.org/10.1016/j.mex.2018.10.002
They write "The equations of transfer of radionuclides in the water and bottom sediment compartments along with the dynamical food chain model are presented." And; (1) 3D compartment model POSEIDON-R describes the transfer of radionuclides and their daughter products in marine environment as results of regular or accidental releases. This includes any transfer through the water column and sediments.
(2) The model is complemented by a dynamic food chain model for transfer of radioactivity in pelagic and benthic food webs.

[17] Y. Inomata, et.al., "Estimate of Fukushima-derived radio Cesium in the North Pacific Ocean in summer 2012", *Journal of Radioanalytical and Nuclear Chemistry* (in printing),
https://link.springer.com/article/10.1007/s10967-018-6249-7, DOI: 10.1007/s10967-018-6249-7.

[18] Kazuo HIIRO, "Eutrophication and red tide occurrence (in Japanese)", *Kankyo Gijyutsu, Soc. of Environmental Conservation Eng*.,vol.20 (12), pp.770-774 (1991). https://www.jstage.jst.go.jp/article/jriet1972/20/12/20_12_770/_pdf.
An index value calculation formula showing the possibility of red tide occurrence is described.

[19] Tsuneo HONJO, "Prediction Techniques of Harmful Red Tides Associated with Fish Kills (in Japanese)",
Bull. Soc. Sea Water Sci. Japan, vol.52 (4), pp.211-215 (1998), https://www.jstage.jst.go.jp/article/swsj1965/52/4/52_211/_pdf.
The cause of red tide is distributed strong winds, which is new knowledge proposed at 1995.

[20] The Earth Observatory is part of the EOS Project Science Office at NASA Goddard Space Flight Center, "Hurricane Isabel Stirs Ocean Water", https://earthobservatory.nasa.gov/images/4480/hurricane-isabel-stirs-ocean-water.

[21] NAVER Conclusions, "The lists of ~ tide like the red tide, or blue tide (in Japanese)",
https://matome.naver.jp/odai/2149822672970811701.

[22] Wikipedia (in Japanese), "thermohaline circulation",
https://ja.wikipedia.org/wiki/%E7%86%B1%E5%A1%A9

%E5%BE%AA%E7%92%B0.

[23] The Environmental Literacy Council, “The Great Ocean Conveyor Belt”, https://enviroliteracy.org/water/oceans/the-great-ocean-conveyer-belt/.
The images are in National Oceanic and Atmospheric Administration (NOAA), “The Global Conveyor Belt”, https://oceanservice.noaa.gov/education/tutorial_currents/05conveyor2.html.

[24] Satoru YOSHIDA, Hidetaka HIRATA, “Ocean vortices and front lines and clarification of atmospheric and ocean phenomena generated by them (in Japanese); *Earth Simulator JAMSTEC Proposed Project*”, https://www.jamstec.go.jp/ceist/j/publication/annual/annual2017/pdf/2project/chapter2/2-11_nonaka.pdf.

[25] Japan Meteorological Agency, “Global Warming and Ocean (in Japanese)”, https://www.data.jma.go.jp/cpdinfo/chishiki_ondanka/p10.html.
More than 90% of thermal energy accumulated throughout the earth during 40 years from 1971 to 2010 is absorbed by the ocean.

[26] Hiroyasu HASUMI, “Ocean General Circulation (in Japanese)”, Atmosphere and Ocean Research Institute (AORI), the University of Tokyo, http://ccsr.aori.u-tokyo.ac.jp/~hasumi/work/ocean_general_circulation.pdf.

[27] Masahiro WATABE, *et.al*., “Investigation of stagnation factors (the hiatus) of global warming, 30% of temperature change in the 2000s is natural variation (in Japanese)”, Atmosphere and Ocean Research Institute (AORI), the University of Tokyo, http://www.aori.u-tokyo.ac.jp/research/news/2014/20140901.html, 2014.9.1.

[28] Toru YAGI, Junko KAMBE, Tomoo AOYAMA, “Detection of invisible SPM distribution in the sky”, *Informatio* (University of Edogawa), vol.14, IN2017-04.pdf, (2017.3.31), https://edo.repo.nii.ac.jp/?action=pages_view_main&active_action=repository_view_main_item_detail&item_id=761&item_no=1&page_id=13&block_id=21.

[29] Tomoo AOYAMA, *et.al*., “Aerosol Distribution in the Atmosphere, Detected at Wavelength Range of 760-1000nm”, *J.Comput.Chem.Jpn.*, vol.8(4), pp.139-152 (2009), https://www.jstage.jst.go.jp/article/jccj/8/4/8_H2101/_article/-char/ja, DOI https://doi.org/10.2477/jccj.H2101.

[30] “Landsat8”, Wikipedia (English), https://en.wikipedia.org/wiki/Landsat_8.

[31] Libra, NASA, https://libra.developmentseed.org/.
“Libra” is a DB that deals with many images, contents are being updated. Old images may disappear. Back up the necessary images for yourself.

[32] Yuji SAKUNO, Ariyo KANNO, Yukio KOIBUCHI, “Simultaneous Estimation of SS and Chlorophyll in Shallow Water through Remote Sensing”, *Proceedings B2(ocean engineering) of Japan Society of Civil Engineers* (JSCE), vol.66(1), pp.1026-1030 (2010).

[33] Akihiko KONDOH, “Vegetation and Land Cover Change Detection by Global Remote Sensing and its Causal Analyses”, *J. Japan Soc. Hydrol. & Water Resour.*, vol.17(5), pp459-467 (2004).

[34] Record China, https://www.recordchina.co.jp/b173237-s0-c30-d0065.html.
The sea foam is generated by the agitation of seawater; where the sea water contains higher concentrations of dissolved organic matters that are proteins, lignins, and lipids. On seacoasts along the Japan Sea, the foam is found in winter; but the event is in the summer, and the area is offshore.
Ozone Monitoring Instrument (OMI) in satellite “Aura” detects the emission of nitrogen dioxide ($NO_2$), and show another sea pollution map. *Cf*. Keith BARRY, “Satellite Image Shows Tracks of Shipping Pollution”, WIRD NEWS, https://www.wired.com/2013/02/satellite-pollution-tracks/. On the map, the south part of the Japan Sea is polluted. The East China Sea is also.